Studies of Elastic Scattering of Protons, Deuterons, and Alpha Particles from Isotopes of Cu, Ni, and Fe*

L. L. Lee, Jr., and J. P. Schiffer

Argonne National Laboratory, Argonne, Illinois

(Received 2 January 1964)

Angular distributions of elastically scattered protons have been measured at bombarding energies of 7, 8, 9, 10, 11, and 12 MeV from enriched isotopic targets of Ni^{58}, Ni^{60}, Cu^{63}, and Cu^{65}. The angular distributions of 12-MeV elastically scattered protons, deuterons, and alpha particles have been measured from targets of Ni^{58}, Ni^{60}, Ni^{62}, Ni^{64}, Cu^{63}, Cu^{65}, and Fe^{54}. The range of angles measured was between 20 and 169°. Absolute cross sections are believed to be accurate to about 5% the relative measurements to 2.5%. The measured angular distributions are compared with ones calculated from optical-model potentials. For the proton scattering, the sensitivity of such data to a symmetry term in the potential and to the dependence of the potential on incident proton energy was also investigated and the results are compared with the ones arrived at by Perey.

INTRODUCTION

THE elastic scattering of charged particles has been studied rather extensively in the last decade. A large volume of data has been accumulated and analyzed in terms of scattering from a complex potential well.[1-4] From the results of such analyses considerable information has been accumulated on the parameters obtained by fitting such a well to the experimental data. This paper makes no attempt to review or summarize preceding work in the field; only the immediately relevant references are quoted. The main deficiency of the earlier work is that most of it was done on fixed-energy accelerators; a study of the energy dependence of the scattering must therefore rely on data obtained at different laboratories where differences in systematic errors might introduce difficulties. There have been relatively few measurements on targets of enriched isotopes: in particular there have been few attempts to measure the elastic scattering from several isotopes of the same element. In an investigation of the optical potential for protons, this sort of information can be of considerable interest in determining the behavior of terms that depend on the neutron excess. The presence of such terms has been suggested by Lane[5] on the basis of the anomalous peak seen in (p,n) reactions,[6] and Perey[1] found it to be necessary in a recent survey of elastic scattering of protons.

The Argonne tandem accelerator provides a variable-energy source of particles for such scattering studies. A remotely controlled scattering chamber made it possible to study the scattering from a number of targets with no change in the experimental conditions. These facilities were utilized to obtain directly compar-

able data for a series of target nuclei and bombarding energies.

EXPERIMENTAL METHOD

The particle beams of the Argonne tandem Van de Graaff accelerator were used in an 18-in. scattering chamber developed by Heinrich and Braid. This chamber was constructed with a remotely controlled arm on which a detector could be mounted and rotated about the target. The angles could be set remotely with a precision better than 0.2°. By means of a remotely controlled target changer, any one of eight targets could be presented to the incident beam. The beam itself was defined by two circular apertures, $\frac{1}{16}$ in. in diameter and 11 in. apart, followed by a slightly larger antiscattering slit.

This collimation system was electrically insulated. The beam intercepted by any collimator was always less than 25% of the beam incident on the target. Silicon diode detectors were used to detect the scattered particles. Targets were thin foils of the enriched isotopes, usually less than 3.5 mg/cm^2 in thickness.

The pulses from the detector were recorded in a 100-channel section of a 400-channel pulse-height analyzer. The contents of the magnetic-core memory of this analyzer could be dumped directly into the memory of an IBM-1620 computer which then punched cards and by means of a digital plotter graphed this information while the next data point was recorded. This introduced considerable saving in analyzer readout time and in setting biases as a function of angle. Thirty-point angular distributions for seven targets could be obtained in this manner in a period of about 6 h.

The data were subsequently analyzed by an IBM-704 computer. The only additional information supplied to the computer was the masses and energies involved in the reaction and a set of channel numbers corresponding to the peaks to be analyzed at one angle. The computer proceeded to subtract background, sum channels, convert to center-of-mass yield, and compute the ratio to Rutherford scattering. For the next spectrum, involving the same target at a new angle, the computer

---

* Work performed under the auspices of the U. S. Atomic Energy Commission.

[1] F. G. Perey, Phys. Rev. 131, 746 (1963).

[2] C. M. Perey and F. G. Perey, Phys. Rev. 132, 755 (1963).

[3] E. C. Halbert (to be published).

[4] R. M. Eisberg and C. E. Porter, Rev. Mod. Phys. 33, 190 (1961).

[5] A. M. Lane, Phys. Rev. Letters 8, 171 (1962).

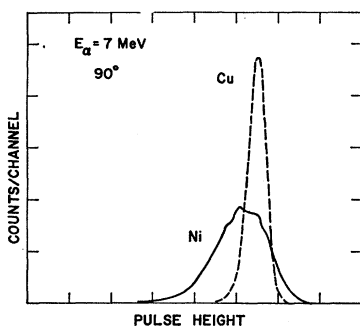[6] J. D. Anderson and C. Wong, Phys. Rev. Letters 7, 250 (1961).

FIG. 1. Pulse-height spectra of alpha particles scattered by foils of Ni and Cu, both about 3.0 mg/cm² thick, observed at 90° in a Si semiconductor counter. The target was at 45° to the incident beam and particles were observed emerging from the side of the foil opposite to the side which was hit by the beam. The beam spot was 0.06 in. in diameter. The difference in shapes indicates a nonuniformity in the Ni foil on a scale smaller than the beam diameter.

calculated the new channels from reaction kinematics and proceeded with the calculation. The output of the computer included a table of angles, center-of-mass differential cross sections, and ratios to Rutherford scattering, as well as graphs for each spectrum (the spectrum with the background subtracted), and the channels over which the spectrum was summed for the various peaks. The program also allows for similar calculations for charged particles from any reaction and for the inclusion of absorbers between the target and the detector.

In obtaining absolute cross sections, considerable care had to be taken because it was found that the Ni foils used were highly nonuniform, even over the small area covered by the beam ($\frac{1}{16}$ in. in diameter). This is illustrated in Fig. 1, where the spectrum of 7-MeV alpha particles scattered at 90° from a Ni target and observed through the foil is compared with the corresponding spectrum for a Cu target of the same thickness. Non-
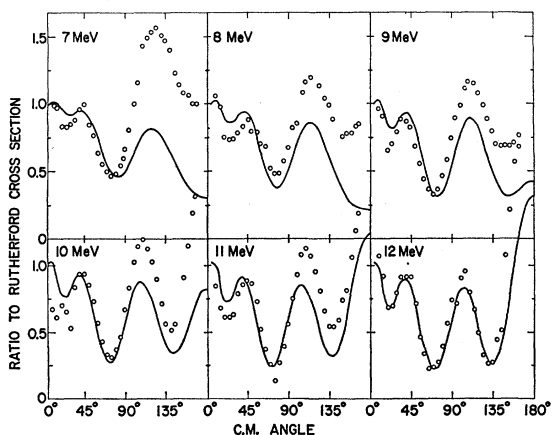
uniformity in the Ni foils means that small variation in the distribution of the beam over the target spot could cause variations in counting rates. Such variations of the order of 10% were in fact observed. It was therefore necessary to keep a monitor counter at a fixed angle and to normalize all other measurements to it.

Because of these nonuniformities, it was also felt that the usual method of weighing the target foils could lead to errors in the absolute cross sections. The target thicknesses were therefore determined by measuring the scattering of the 7-MeV alpha particles at 90° and assuming that these were scattered by the Coulomb field only. The calculation of this scattering for reasonable optical-model parameters indicates that the scattering differs from Rutherford scattering by less than 0.7%. The target thickness was then determined over the beam area by an iterative calculation allowing for the variation of the stopping power and the Rutherford cross section over the relatively thick targets. For these measurements the beam was kept deliberately

FIG. 3. Ratio of elastic-scattering cross section to Rutherford cross section as a function of angle for protons incident on Cu⁶⁵. The theoretical curve is calculated for a potential suggested by Perey.

defocused in order to insure a uniform distribution over the target spot.

Without any change within the target chamber, a beam of protons was obtained immediately after the alpha particles and the yield of scattered protons was determined without moving the target or detectors and for the same amount of integrated beam charge. The cross sections obtained in this way were found to be reproducible within the stated experimental errors. Special precautions had to be taken to insure correct integration of the beam current. A permanent magnet placed near the opening of the Faraday cup and a 600-V suppressor grid placed between the target and the Faraday cup were found to be adequate.

DISCUSSION

A. Elastic Scattering of Protons

The measured cross sections divided by the Rutherford cross section are tabulated in Tables III-VII in
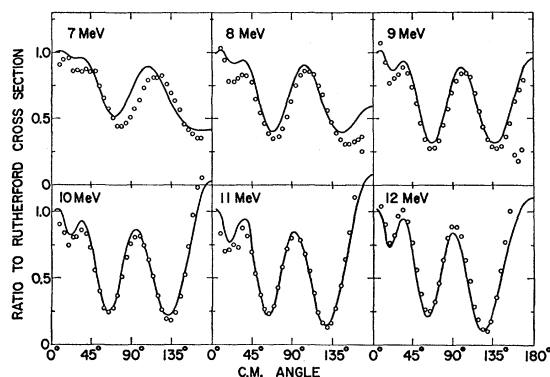

FIG. 2. The ratio of elastic-scattering cross sections to Rutherford cross section as a function of angle for protons incident on Ni⁵⁸. The theoretical curve is calculated for a potential suggested by Perey.

TABLE I. Parameters of the optical-model potentials
used in calculating theoretical curves.

Incident particle	V_S (MeV)	r_{0S} (F)	a_S (F)	W_S (MeV)	r_{0I} (F)	a_I (F)	V_{S0} (MeV)
Protons[a]	53.3[b]	1.25	0.65	13.0	1.25	0.47	7.5
Deuterons[c]	57.4	1.15	0.87	17.6	1.37	0.7	
Deuterons[c]	92.0	1.15	0.81	23.7	1.39	0.68	
Deuterons[c]	167.8	1.232	0.72	31.9	1.395	0.56	
Alpha particles[d]	49.5	1.35[e,f]	0.50[f]	11.0[f]			

[a] See Ref. 1.
[b] The real potential depth is taken as $53.3-0.55E+0.4Z/A^{1/3}+27(N-Z)/A$ MeV.
[c] See Ref. 2.
[d] See Ref. 4.
[e] The radius is in the form $(1.35A^{1/3}+1.3)$ F.
[f] The imaginary potential has the same shape and radial parameters as the real potential (volume absorption).

the Appendix. Figures 2 and 3 show the results obtained for Ni[58] and Cu[65] at the various energies used. The theoretical curves are those calculated for optical-model parameters (Table I) suggested by Perey.[1] The shape of the potential is the usual Woods-Saxon shape with surface absorption

$$V = -V_S f(r,r_{0S},a_S)+iW_S 4a_I(d/dr)f(r,r_{0I},a_I),$$

where

$$f(r,r_0,a)=\{1+\exp[(r-r_0A^{1/3})/a]\}^{-1}.$$

The relatively poor agreement at the lower energies in Ni[58] can probably be attributed to the large fluctuations in the cross sections as a function of energy. These are shown in Fig. 4 where the excitation functions at 90° are compared for various targets.

It is of interest to note that the fluctuations in the excitation functions seem to disappear about 2 MeV above the (p,n) threshold for both Ni isotopes. It is likely that at these energies at least 10 channels will be open for neutron emission. The detailed study of the observed fluctuations has been discussed in an earlier publication[7] in which it was pointed out that they are in the nonrandom clustering of many narrow resonances and are probably associated with residual single-particle or gross-structure effects. Since an optical model obviously cannot reproduce these effects, it is clear that the scattering will deviate from the predicted shape at energies where such effects are strong. It is also clear that no simple correction for compound-nucleus scattering is justified, since presumably the resonances occur in different partial waves, each of which has a different effect on the angular distributions.

Since the measured cross sections agree reasonably well with the calculated ones, except as mentioned above, it was thought to be worthwhile to investigate two of the terms in the optical potential suggested by Perey,[1] namely a term that changes with neutron excess and a term that depends on proton kinetic energy.

The search for these effects requires a rather careful analysis, since effects are rather small because of the limited region of energy and neutron excess. The
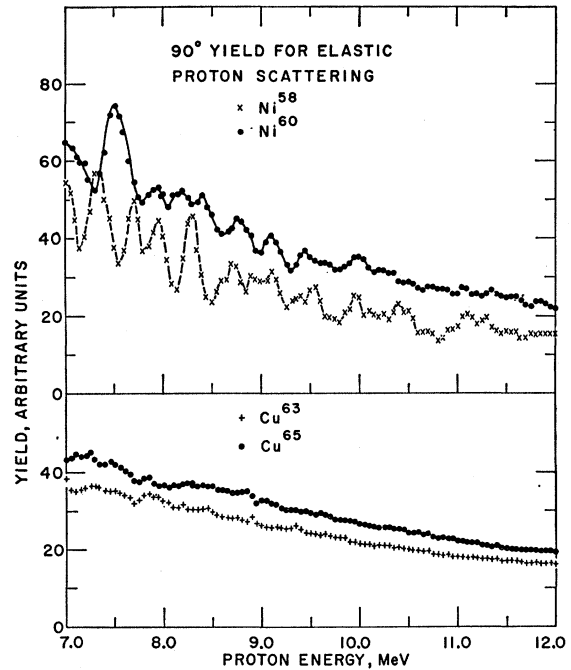
FIG. 4. Excitation functions for elastic scattering at 90°. The targets were about 100 keV thick.

angular distributions will change because of changing radius or kinetic energy in any case, and the measurements usually do not fit the calculated curves exactly. We have therefore attempted to display the data in a form which emphasizes only the change in the angular distributions, so that this can be compared with the calculated change. The ratio of cross sections does not quite fulfill this requirement because the cross sections change with energy and charge (because of the changes in Coulomb scattering). It was therefore decided that the data were best displayed in the form of the ratios of two cross sections, each of which is divided by the Rutherford cross section for its respective energy and
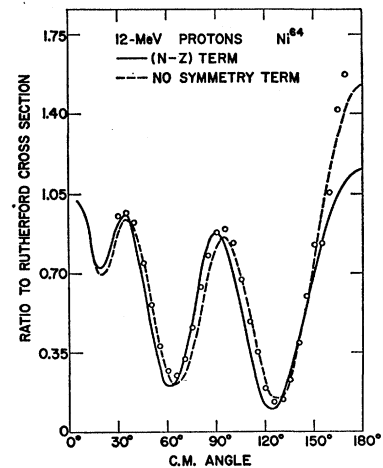
FIG. 5. Elastic-scattering cross section of 12-MeV protons from Ni[64], expressed as the ratio to the Rutherford cross section. The two theoretical curves are for the Perey potential and for a potential which differs from this only in that its depth is the same for Ni[64] as for Ni[58].
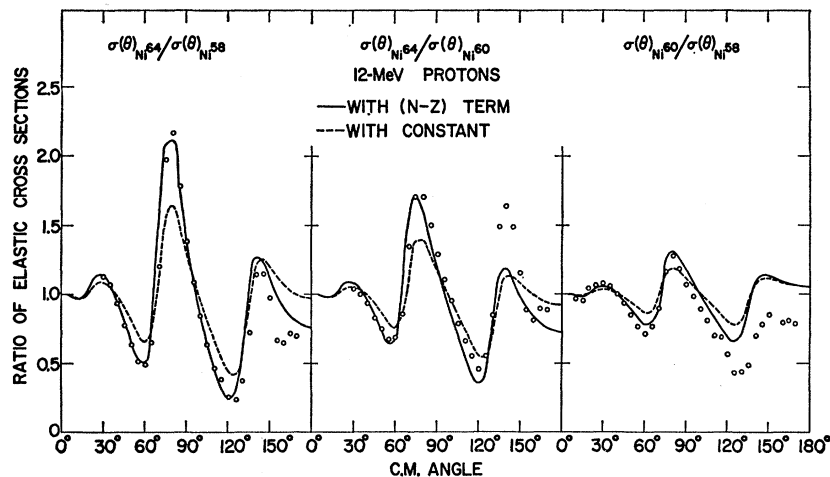
FIG. 6. Ratios of elastic-scattering cross sections of 12-MeV protons from various pairs of Ni isotopes. The theoretical curves are for the Perey potential and for a potential which differs from this only in that the depth is kept the same for each isotope.

charge. Such ratios are particularly sensitive to small shifts in the positions of the maxima and minima of the angular distributions.

The importance of the form of display is illustrated by Figs. 5 and 6. In Fig. 5, the elastic scattering from Ni^{64} is compared with two theoretical curves, one containing the symmetry term and one not. While it is clear that qualitatively the agreement is better with the angular distribution which contains a symmetry term, it is hard to form a more quantitative evaluation of the result. At the left in Fig. 6 is a plot of the same results divided by the cross sections for Ni^{58}. It is clear that the small shift in the angular distributions is now strongly emphasized; the shift in the diffraction pattern is definitely larger than would be predicted only from the increase in radius. The additional observed shift in the potential well has about the magnitude calculated by Perey. Figure 6 also includes similar plots comparing Ni^{64} with Ni^{60} and Ni^{60} with Ni^{58}. The agreement in the latter two cases in not quite so good. The differences probably are attributable to the small differences between the effective optical-model potentials of neighbor-

ing nuclei. Such differences might be due to small details of the structure of these particular nuclei. Figure 7 shows a similar plot comparing Ni^{64} with Cu^{63}. From these comparisons, we can thus conclude that the potential contains the symmetry term and that the magnitude of the term agrees well with that calculated by Perey. Similar conclusions have been reached by Benveniste, Mitchell, and Fullmer,[8] who compared the scattering by different isobars. Their data on Ni^{58} and Ni^{64} at 11.7 MeV are in excellent agreement with the present work at 12 MeV.

The energy-dependent term in the potential was likewise studied. This term, which Perey found to be necessary in fitting the data, represents the local equivalent of a nonlocal potential. Figure 8 shows the ratios of cross sections for proton scattering from Cu^{63} at various energies. The theoretical curves are for potentials with and without the energy-dependent term. Below 9 MeV there is no significant difference between the two theoretical curves; but above it seems that the data are fitted slightly better without the energy-dependent term. However, the disagreement between the data and either theoretical curve is greater than the difference between the two theoretical curves. Figure 9 shows the ratio of the scattering cross sections at two more widely separated energies for this nuclide and also for Ni^{60} and Cu^{65}. Our data point to no clear conclusion about the energy dependence found by Perey. Possibly the effects of this term became important only at incident energies higher than 12 MeV.

B. Deuteron Scattering

Angular distributions of 12-MeV deuterons elastically scattered from all the targets were also obtained, but again no fitting was attempted. A recent paper by Perey and Perey[2] contains an exhaustive and systematic
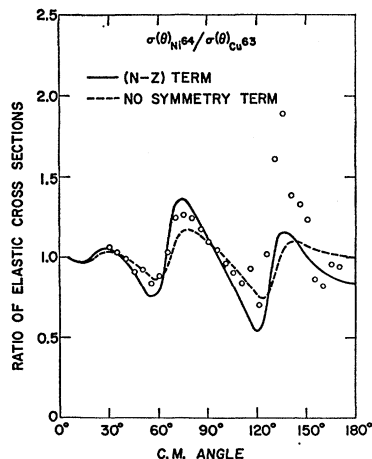
FIG. 7. Ratio of cross section of Ni^{64} to that of Cu^{63}. The theoretical curves are calculated in the same way as for Fig. 6.

[7] L. L. Lee, Jr., and J. P. Schiffer, Phys. Letters 4, 104 (1963).
[8] J. Benveniste, A. C. Mitchell, and C. B. Fullmer, Phys. Rev. 129, 2173 (1963); 133, B317 (1964).

analysis of the data on elastic scattering of deuterons. Figure 10 shows that three potentials which they used in fitting the Cu data fit equally well for Ni[62]. The data presented here (Table VIII of the Appendix) seem to be fitted best by the deepest well, but this is probably fortuitous; it is likely that with small adjustments of their parameters, equally good fits can be obtained with the other wells.

Figure 11 compares the data from Ni[58] with that from Ni[64]. For deuterons one would not expect to find a symmetry term in the potential since its isotopic spin is zero. If one therefore requires that the increase in radius R alone should explain the shift in the diffraction pattern, then it is clear that only the deepest well fits the observed magnitude reasonably well. The reason is that the positions of the diffraction maxima and minima depend on KR, where K is the deuteron wave number inside the nucleus, and the increasing well depths correspond to successively fitting an additional half-wavelength into the well.[9] A larger number of wavelengths fitting into the well will increase the rate at which the angular-distribution pattern will shift with increasing radius. It may then perhaps be argued, although the evidence is weak, that a deeper well (roughly 167 MeV) may fit the data better. However, if the optical model for a deuteron is treated as a purely phenomenological device for fitting data, then it is clearly meaningless to prefer one set of potentials over another when both fit the data equally well. Only if one imposes the requirement that the well parameters shall not change from nucleus to nucleus (or that the change must be as small as possible) can one perhaps choose one set over another.
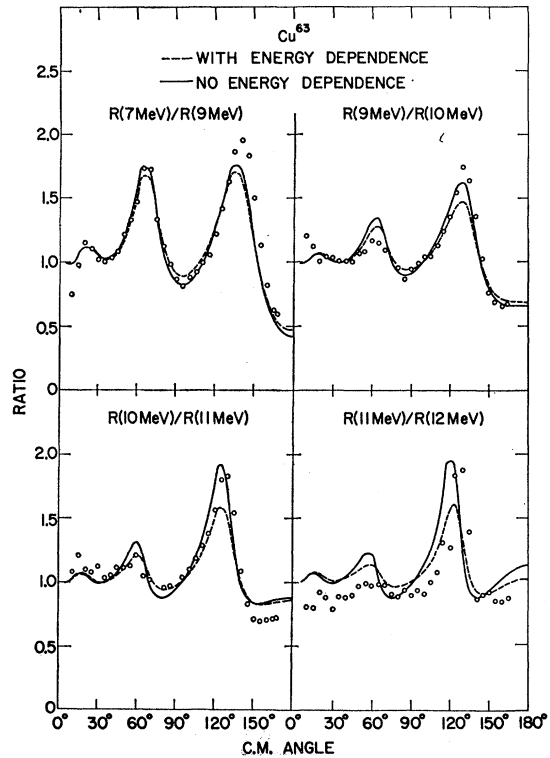
FIG. 8. Ratios of cross sections divided by the Rutherford cross sections at various energies for Cu[63]. The theoretical curves are calculated with and without the energy-dependent term in the Perey potential.

C. Alpha-Particle Scattering

The cross sections for elastic scattering of 12-MeV alpha particles were also obtained and are given in
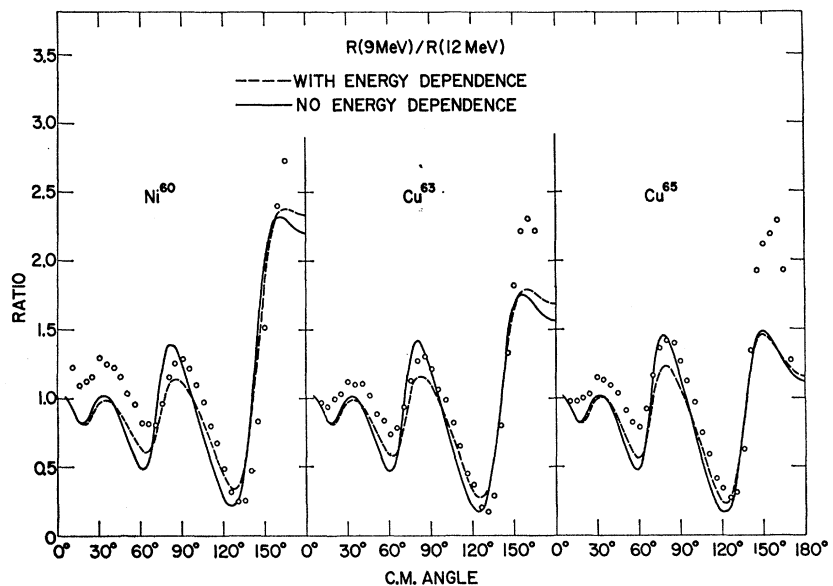
FIG. 9. Ratio of elastic cross sections to Rutherford cross sections at 12 MeV divided by the corresponding ratio at 9 MeV for Ni[60], Cu[63], and Cu[65]. The theoretical curves are calculated in the same manner as in Fig. 8.

[9] R. M. Drisko, G. R. Satchler, and R. H. Bassel, Phys. Letters 5, 347 (1963).
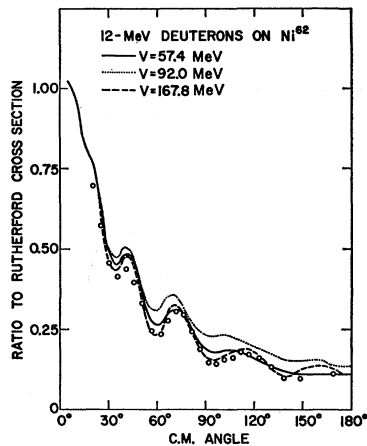
FIG. 10. Ratio of elastic-scattering cross section to Rutherford cross section for deuterons scattered from Ni⁶². The theoretical curves are for three potentials given in Table I.
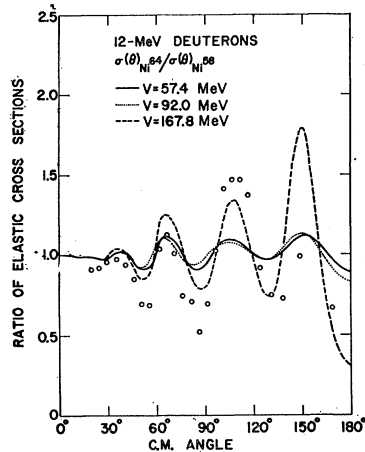
FIG. 11. The ratio of elastic deuteron cross sections for Ni⁶⁴ and Ni⁵⁸. The theoretical curves are for the three potentials given in Table I.
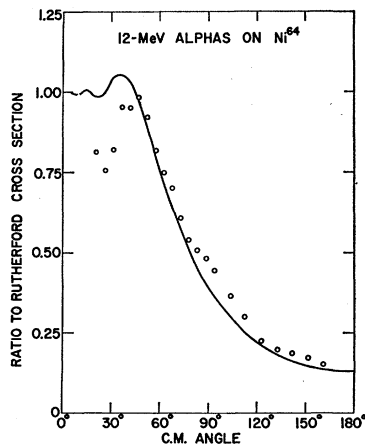
FIG. 12. Ratio of elastic-scattering cross section to Rutherford cross section for 12-MeV alpha particles scattered from Ni⁶⁴. The potential used to calculate the theoretical curve is given in Table I.

FIG. 13. Inelastic scattering of 12-MeV protons to the 2⁺ first excited states of the Ni isotopes. The errors in the cross sections are less than 15%.

D. Inelastic Scattering of Protons

The inelastic scattering to the 2⁺ first excited states of the four Ni isotopes was also measured at 12 MeV. These results are shown in Fig. 13. Since the inelastic cross sections were not measured as accurately as the elastic and since the inelastic peak was in fact obscured by impurities at several angles, these data are only shown in the figure and are not included in the Appendix. It is interesting to observe that while the shapes are very similar, the absolute cross sections vary considerably. Table II compares known values[10] of $B(E2)$ and

TABLE II. Comparison of cross sections for inelastic scattering of 12-MeV protons to 2⁺ first excited states and reduced transition probabilities.

Nucleus	$B(E2)$ of first 2⁺ state[a] (10^{-49} cm^4)	$\sigma(90°)-\sigma(100°)$[b] (mb/sr)
Ni⁵⁸	0.72	5.1
Ni⁶⁰	0.92	3.3
Ni⁶²	0.83	2.9
Ni⁶⁴	0.87[c]	2.8

[a] See Ref. 10.
[b] Average inelastic cross section at these angles.
[c] D. S. Andreyev, A. P. Grinberg, K. I. Erokhina, and I. Kh. Lemberg, Nucl. Phys. 19, 400 (1960).

relative cross sections. It is hoped that these data may be analyzed in more detail in terms of coupled potentials.[11] The relatively large cross section for Ni⁵⁸ can perhaps be attributed to a more significant compound-inelastic contribution.

APPENDIX

The experimental cross sections are listed in Tables III–IX. In order to allow cross sections for various isotopes to be listed in the same table, laboratory angles are given in some cases rather than center-of-mass ones.

Table IX of the Appendix. The data for Ni⁶⁴ are displayed in Fig. 12 with a theoretical curve calculated with the parameters that Eisberg and Porter[4] obtained for 40-MeV α particles scattered from Cu. The fit is reasonably good, except for forward angles. Since the curve is rather featureless, it is perhaps questionable to what extent such low-energy data (the Coulomb barrier is 14 MeV) are sensitive to the details of optical-model parameters.

[10] P. H. Stelson and F. K. McGowan, Nucl. Phys. 32, 652 (1962).
[11] B. Buck, Phys. Rev. 130, 712 (1963).

TABLE III. Elastic cross sections for scattering of protons at 12 MeV.

Laboratory angle (degrees)	Center-of-mass differential cross sections (mb/sr)[a]						
	Fe^{54}	Ni^{58}	Ni^{60}	Ni^{62}	Ni^{64}	Cu^{63}	Cu^{65}
20.0		5470.00	5730.00			5970.00	6210.00
25.0		2310.00	2470.00			2650.00	2780.00
30.0	1030.00	1310.00	1410.00	1530.00	1470.00	1480.00	1580.00
35.0	695.00	770.00	817.00	782.00	822.00	859.00	914.00
40.0	454.00	500.00	501.00	462.00	467.00	507.00	501.00
45.0	290.00	310.00	291.00	259.00	240.00	283.00	265.00
50.0	186.00	192.00	163.00	133.00	122.00	141.00	131.00
55.0	115.00	112.00	86.00	68.00	58.00	74.00	63.00
60.0	65.30	61.00	43.60	33.30	30.10	36.50	32.20
65.0	35.60	32.20	24.60	19.80	21.10	21.90	22.60
70.0	18.60	17.40	15.50	17.20	20.90	18.00	22.20
75.0	10.39	11.77	13.68	18.00	23.30	19.76	25.00
80.0	8.71	12.10	15.41	20.50	26.24	22.55	28.21
85.0	10.79	14.69	17.45	22.49	26.24	23.92	29.05
90.0	14.13	17.92	19.15	22.35	24.72	24.28	26.82
95.0	16.47	19.83	19.47	20.45	21.46	22.05	22.65
100.0	18.10	20.20	18.00	17.00	17.10	19.10	17.90
105.0	17.93	19.06	15.28	12.80	12.06	14.31	12.21
110.0	16.49	16.57	11.52	8.77	7.67	9.79	8.12
115.0	13.56	12.94	8.93	5.59	4.93	5.71	4.29
120.0	10.45	9.48	5.33	3.15	2.43	3.72	2.59
125.0	7.56	6.56	2.78	1.47	1.54	1.62	1.50
130.0	5.10	4.09	1.77	1.25	1.50	1.00	1.23
135.0	4.44	3.15	1.53	1.79	2.27	1.22	1.90
140.0	4.46	3.16	2.21	2.93	3.61	2.78	3.64
145.0	5.76	4.55	3.53	4.80	5.22	4.21	5.25
150.0	7.21	7.04	5.93	6.91	6.85	5.95	6.94
155.0	9.48	9.97		6.17	6.64	8.30	8.61
160.0	11.41	12.59	9.98	11.13	8.14	10.61	11.79
165.0	11.74	14.86	11.91	12.36	10.65	11.98	11.18
169.5	14.20	16.78	13.12	13.78	11.63	13.24	11.69

[a] The errors in the cross sections are estimated to be ±5% except for $\theta \leq 25°$ where they are ±10%.

TABLE IV. Elastic cross sections for scattering of protons from Ni^{58} at 7, 8, 9, 10, and 11 MeV.

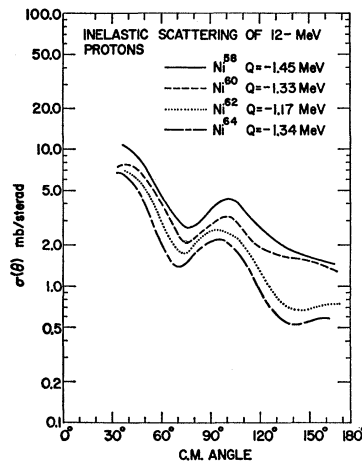| Center-of-mass angle (degrees)	Differential cross section (mb/sr)[a]				
	7 MeV	8 MeV	9 MeV	10 MeV	11 MeV
20.34	18300.00	12800.00	8900.00	7600.00	5500.00
25.42	7590.00	5130.00	3650.00	2950.00	2290.00
30.49	3810.00	2540.00	1900.00	1150.00	1160.00
35.57	2300.00	1490.00	1190.00	1010.00	800.00
40.63	1426.00	943.00	789.00	674.00	511.00
45.70	941.00	634.00	497.00	433.00	339.00
50.76	537.00	386.00	319.00	266.00	223.00
55.81	343.00	274.00	187.00	161.00	132.00
60.86	206.00	176.00	110.00	92.00	69.00
65.90	136.70	114.30	66.20	51.90	37.30
70.93	96.10	76.40	41.60	30.90	19.70
75.95	69.40	55.90	29.10	22.80	8.30
80.97	58.10	45.20	26.90	21.90	12.90
85.98	54.30	43.50	28.10	22.80	15.80
90.99	55.30	42.70	29.30	26.70	18.90
95.98	57.30	44.50	31.80	28.70	21.60
100.97	61.10	39.70	32.80	30.40	23.00
105.95	61.50	43.90	31.50	29.60	23.10
110.93	62.10	41.70	31.40	27.30	21.20
115.90	57.80	38.20	29.30	23.00	18.00
120.86	53.80	34.50	26.00	18.90	14.50
125.81	50.20	29.80	22.30	15.00	11.10
130.76	44.60	25.10	18.80	11.00	8.30
135.70	40.10	21.40	15.70	8.00	6.40
140.63	35.60	18.50	13.20	7.00	6.00
145.57	31.80	15.90	11.00	7.20	6.20
150.49	28.10	14.30	10.10	8.10	7.40
155.42	25.60	14.20	9.80	10.50	8.80
160.34	24.30	13.80	9.50	12.70	9.90
165.26	22.20	14.20	9.60	15.20	11.30
168.21	22.00	14.40	10.20	16.40	12.40

[a] The errors in the cross sections are estimated to be ±5% except for $\theta \leq 25°$ where they are ±10%.

TABLE V. Elastic cross sections for scattering of protons from Ni^{60} at 7, 8, 9, 10, and 11 MeV.

Center-of-mass angle (degrees)	Differential cross section (mb/sr)[a]				
	7 MeV	8 MeV	9 MeV	10 MeV	11 MeV
20.33	19200.00	12600.00	9000.00	7700.00	6200.00
25.40	7790.00	5020.00	3780.00	3070.00	2650.00
30.48	3700.00	2490.00	1930.00	1690.00	1300.00
35.55	2150.00	1480.00	1160.00	1020.00	850.00
40.61	1286.00	917.00	724.00	631.00	529.00
45.68	830.00	584.00	448.00	383.00	315.00
50.73	493.00	347.00	280.00	226.00	191.00
55.78	319.00	225.00	160.00	127.00	103.00
60.83	210.00	126.00	94.00	66.00	53.00
65.87	136.50	84.00	53.40	37.80	29.50
70.90	98.20	62.00	34.30	23.90	18.00
75.92	70.60	53.60	25.20	21.40	15.60
80.94	58.30	51.20	23.80	22.10	16.80
85.95	52.40	47.90	24.70	24.60	19.00
90.95	48.90	49.10	26.50	27.60	21.50
95.95	47.50	48.20	28.60	29.10	21.60
100.94	48.10	47.40	29.10	27.40	20.50
105.92	49.30	44.60	27.80	25.50	18.50
110.90	48.60	41.00	25.60	22.10	15.30
115.87	46.20	36.00	23.40	18.20	11.50
120.83	45.60	31.20	19.30	13.70	8.40
125.78	43.60	27.10	15.60	10.40	5.90
130.73	40.50	22.70	12.80	9.90	4.00
135.68	37.70	18.50	10.70	5.20	3.20
140.61	35.10	15.80	8.30	4.30	3.50
145.55	32.80	13.60	7.50	4.30	4.80
150.48	30.60	12.60	7.00	4.90	6.50
155.40	29.80	11.40	7.00	6.20	8.40
160.33	28.90	11.20	7.40	7.60	11.10
165.25	26.60	10.90	7.80	9.10	13.50
168.20	26.60		8.00	10.10	14.70

[a] The errors in the cross sections are estimated to be ±5% except for $\theta \leq 25°$ where they are ±10%.

TABLE VI. Elastic cross sections for scattering of protons from Cu^{63} at 7, 8, 9, 10, and 11 MeV.

Center-of-mass angle (degrees)	Differential cross section (mb/sr)[a]				
	7 MeV	8 MeV	9 MeV	10 MeV	11 MeV
20.31	20500.00	13900.00	10700.00	8500.00	6500.00
25.38	8320.00	5590.00	4540.00	3550.00	2730.00
30.45	3970.00	2860.00	2350.00	1860.00	1370.00
35.52	2290.00	1640.00	1380.00	1110.00	890.00
40.58	1390.00	965.00	815.00	661.00	520.00
45.64	881.00	601.00	489.00	396.00	296.00
50.70	524.00	343.00	282.00	215.00	160.00
55.74	342.00	213.00	156.00	117.00	86.00
60.79	213.00	135.00	87.00	60.00	41.00
65.82	141.00	85.30	49.10	35.00	25.30
70.85	97.20	58.50	34.10	25.30	20.60
75.88	68.30	45.90	31.00	24.30	20.90
80.90	58.40	42.70	31.40	27.00	23.40
85.91	52.90	43.30	32.50	30.40	26.10
90.91	50.50	42.70	35.40	30.50	25.60
95.91	49.20	42.90	36.70	30.00	24.00
100.90	49.60	41.80	34.30	26.90	20.40
105.88	47.00	38.70	30.80	24.00	16.70
110.85	43.70	36.10	26.40	19.10	12.30
115.82	39.20	31.60	22.40	14.60	8.80
120.79	35.50	27.30	17.60	10.60	5.60
125.74	32.20	22.50	13.70	7.20	3.30
130.70	26.80	18.40	10.00	4.60	2.10
135.64	23.30	13.80	7.50	3.70	2.00
140.58	19.70	11.10	6.10	3.70	2.80
145.52	17.01	8.84	5.60	4.45	4.44
150.45	14.39	7.19	5.80	6.18	6.37
155.38	12.49	6.61	6.67	7.87	8.22
160.31	11.04	6.36	8.19	10.18	10.48
165.24	9.88	6.60	9.64	11.83	12.20
168.19	9.75	6.80	10.12	13.28	13.40

[a] The errors in the cross sections are estimated to be ±5% except for $\theta \leq 25°$ where they are ±10%.

TABLE VII. Elastic cross sections for scattering of protons from Cu^{65} at 7, 8, 9, 10, and 11 MeV.

Center-of-mass angle (degrees)	Differential cross section (mb/sr)[a]				
	7 MeV	8 MeV	9 MeV	10 MeV	11 MeV
20.30	20300.00	14400.00	11000.00	8700.00	6900.00
25.37	8550.00	5920.00	4790.00	3870.00	3030.00
30.44	4150.00	2970.00	2430.00	1900.00	1430.00
35.51	2320.00	1700.00	1430.00	1120.00	940.00
40.37	1356.00	1002.00	810.00	649.00	521.00
45.62	870.00	602.00	454.00	362.00	288.00
50.68	512.00	344.00	254.00	186.00	148.00
55.72	315.00	202.00	135.00	95.00	74.00
60.76	202.00	124.00	72.00	47.00	37.00
65.80	133.80	78.10	43.90	31.10	24.70
70.83	91.50	54.10	33.90	27.00	24.40
75.85	71.10	44.60	32.60	29.80	27.70
80.87	61.00	42.30	35.40	32.40	30.30
85.88	54.40	41.90	36.90	34.10	30.80
90.88	51.60	43.00	37.60	32.80	28.70
95.88	48.80	43.40	35.70	29.90	25.00
100.87	47.90	41.10	32.80	25.90	20.70
105.85	45.00	37.30	29.10	20.70	15.70
110.83	40.70	32.60	24.60	15.80	11.20
115.80	36.40	28.40	18.70	11.30	7.00
120.76	33.50	23.10	13.50	7.50	4.10
125.72	27.70	19.10	9.70	4.80	2.40
130.68	23.40	14.50	7.00	3.30	1.80
135.62	20.00	11.30	5.40	2.80	2.10
140.57	16.46	8.78	4.82	3.56	3.28
145.51	14.04	7.29	4.85	4.88	5.04
150.44	11.99	6.18	5.85	6.76	6.86
155.37	10.54	5.96	7.01	9.13	8.56
160.30	9.35	6.10	9.19	11.63	10.90
165.23	8.37	6.07	10.34	13.78	12.48
168.18	8.25	6.61	11.28	14.41	13.84

[a] The errors in the cross sections are estimated to be ±5% except for $\theta \leq 25°$ where they are ±10%.

TABLE VIII. Elastic cross sections for scattering of deuterons at 12 MeV.

Laboratory angle (degrees)	Center-of-mass differential cross sections (mb/sr)[a]					
	Ni[58]	Ni[60]	Ni[62]	Ni[64]	Cu[63]	Cu[65]
20.0	5700.00	5590.00	5090.00	5200.00	5910.00	5920.00
25.0	1910.00	1930.00	1740.00	1750.00	2100.00	2160.00
30.0	706.00	725.00	676.00	676.00	824.00	805.00
35.0	354.00	362.00	342.00	346.00	410.00	390.00
40.0	235.00	238.00	216.00	222.00	242.00	234.00
45.0	149.00	145.00	124.00	127.00	141.00	132.00
50.0	87.10	81.20	69.10	60.70	75.20	66.60
55.0	44.50	40.50	36.10	30.60	41.00	38.10
60.0	21.90	23.30	24.00	22.80	27.60	26.80
65.0	19.60	21.40	22.40	22.20	25.60	25.80
70.0	18.40	19.20	19.60	18.60	21.60	18.90
75.0	15.55	16.50	14.86	11.63	15.33	15.17
80.0	12.73	11.52	9.86	8.99	10.10	8.65
85.0	8.78	7.80	6.25	4.52	6.51	5.42
90.0	5.63	4.97	4.20	3.89	4.56	4.02
95.0	3.25	2.92	3.38	3.35	3.63	3.65
100.0	2.50	2.50	3.13	3.52	3.64	3.98
105.0	2.34	2.41	2.93	3.44	3.45	4.15
110.0	2.20	2.22	2.77	3.22	3.48	3.49
115.0	1.94	2.17	2.45	2.65	2.99	2.69
122.5	1.93	1.61	1.96	1.76	2.15	2.03
130.0	1.65	1.34	1.42	1.23	1.31	1.37
137.5	1.37	1.15	0.91	0.99	1.00	1.00
148.0	1.08	0.97	0.82	1.06	0.95	1.05
168.5	1.89	1.27	0.88	1.25	0.95	0.98

[a] The errors in the cross sections are estimated to be ±5% except for $\theta \leq 25°$ where they are ±10%.

TABLE IX. Elastic cross sections for scattering of alphas at 12 MeV.

Laboratory angle (degrees)	Center-of-mass differential cross sections (mb/sr)[a]			
	Ni[58]	Ni[60]	Ni[62]	Ni[64]
20.0	25300.00	28600.00	28700.00	22500.00
25.0	10600.00	11400.00	11900.00	8700.00
30.0	5410.00	5990.00	6020.00	4640.00
35.0	3200.00	3350.00	3550.00	2980.00
40.0	1960.00	2060.00	2120.00	1790.00
45.0	1280.00	1380.00	1410.00	1190.00
50.0	837.00	882.00	925.00	758.00
55.0	557.00	590.00	622.00	474.00
60.0	379.00	392.00	422.00	318.00
65.0	271.00	277.00	301.00	225.00
70.0	189.00	202.00	214.00	151.00
75.0	140.00	145.00	155.00	107.00
80.0	99.00	105.00	112.00	82.00
85.0	73.20	79.00	84.20	64.80
90.0	57.10	63.90	66.40	50.30
100.0	38.10	40.70	42.40	30.60
110.0	27.60	27.40	26.70	19.50
120.0	18.70	20.10	19.80	11.90
130.0	15.87	15.71	15.45	8.87
140.0	14.75	13.61	12.52	7.48
150.0	12.81	11.61	10.37	6.21
160.0	13.95	12.06	8.96	5.13

[a] The errors in the cross sections are estimated to be ±5% except for $\theta \leq 25°$ where they are ±10%.

ACKNOWLEDGMENTS